Pareto Frontiers of Sensor Networks for Localization

Volkan Cevher*
Rice University, volkan@rice.edu

Lance Kaplan
ARL, lkaplan@ieee.org

Abstract

We develop a theory to predict the localization performance of randomly distributed sensor networks consisting of various sensor modalities when only a constant active subset of sensors that minimize localization error is used for estimation. The characteristics of the modalities include measurement type (bearing or range) and error, sensor reliability, FOV, sensing range, and mobility. We show that the localization performance of a sensor network is a function of a weighted sum of the total number of each sensor modality. We also show that optimization of this weighted sum is independent of how the sensor management strategy chooses the active sensors. We combine the utility objective with other objectives, such as lifetime, coverage and reliability to determine the best mix of sensors for an optimal sensor network design. The Pareto efficient frontier of the multi objectives are obtained with a dynamic program, which also accommodates additional convex constraints.

1 Introduction

Beginning late 90's, there has been an ever-growing interest in sensor networks research, where a large number of sensors are networked *wirelessly* to tackle larger sensing problems in a bandwidth constrained and distributed manner. New hardware technologies, communications, signal processing, and optimization algorithms have been developed to increase the sensing capabilities and lifetime of sensor networks while simultaneously decreasing their cost. As of now, a staggering amount of sensor choices and sensor network management strategies is commercially available.

In this paper, we develop a localization utility for the sensor network design problem, which entails three entangled aspects: sensor choices, operational choices, and deployment plans. Given how the sensor network is operated and how it is deployed, the sensor choices involve the budget allocation in purchasing different sensors with varying costs and capabilities. On the other hand, given the available sensors and a deployment plan, the operational aspect of the design concerns how the sensor network is run and managed, e.g., by using distributed sensor-to-sensor communication and data fusion schemes [11, 18] and algorithms for dynamic assignment of a subset of sensors for parameter estimation to preserve network energy [12, 17]. Finally, the sensor network deployment strategy is related to the actual emplacement of the sensors in the deployment area, e.g., to maximize coverage and visibility [10, 15] and can understandably affect as well as be affected by the sensor choices and how one operates the sensors depending on the knowledge of the geometry and the conditions of the deployment area (e.g., locations of occluders and weather).

We build upon our previous work in [7] to determine the sensor choices for acoustic sensor network design. In [7], the network is composed of different sensors where each sensor is one of T possible sensor types (or modalities). Each sensor type is characterized by a number of performance parameters. Then, under a limited budget \$, sensor network design determines a design vector $\boldsymbol{n} = [n_1,\ n_2, \ldots, n_T]'$, whose elements consists of the number of sensors of type-t ($t = 1, \ldots, T$) to deploy given that each sensor type has a cost c_t. For generality, a random deployment strategy over the surveillance region $\mathcal{A}$ is used. In [7], various objectives such as localization utility, lifetime, and coverage were defined and convex optimization solutions were provided to determine the Pareto frontier for the multiple objectives.

In this paper, different from [7], we consider how the operational aspects of the sensor network affect the localization performance. We identify a duality of range and bearing sensors where for any given range (bearing) sensor, there exists a dual bearing (range) sensor that results in the same average localization performance under random deployment. Subsequently, the localization performance is analytically related to a functional whose argument is a weighted sum of the total number of each sensor type when only a constant number of sensors is activated per period to minimize localization error for energy conservation. To our knowledge, no such formula has been derived before. In contrast, [7] uses all sensors within sensing range for localization and approximates the localization utility by fitting models to network simulation results. Compared to [7], we also account for additional sensor characteristics such as limited field-of-view (FOV), sensor reliability, and mobility. We assess the performance equivalence of mobile sensors and the stationary sensors when mobile sensors use

*Corresponding author.

978-0-7695-3157-1/08 $25.00 © 2008 IEEE
DOI 10.1109/IPSN.2008.8

random walk that preserves their distribution. We emphasize that this paper investigates the effects of sensor mobility on the average network localization performance as opposed to its effects on the sensor network coverage. Hence, mobile sensors operating in a tracking mode is beyond the scope of this paper. Finally, the new localization utility is combined with the design tools developed in [7] to determine how to choose the sensor types for a given budget to trace the Pareto efficient frontier of multiple objectives such as sensor network utility, lifetime, coverage, etc.

The paper is organized as follows. Section 2 describes the sensor network geometry and defines the common variables used in the paper. The sensor design tools are reviewed in Section 3, and the sensor characteristics and resulting localization performance are described in Section 4. Section 5 derives the localization performance and corresponding utility for a heterogeneous network of stationary and mobile nodes that exploits sensor management. Section 6 provides simulations to validate the theoretical performance characterization and to demonstrate the sensor network design. Finally, concluding remarks are provided in Section 7.

2 Deployment Geometry and Notational Preliminaries

For generality, random sensor deployment is assumed so that sensor locations are distributed via a uniform distribution over a surveillance area $\mathcal{A}$ of size A. We ignore the boundary effects by assuming that $\mathcal{A}$ is sufficiently large and toroidal. The location of the ith node is given in Cartesian coordinates as $\boldsymbol{\zeta}_i = (\zeta_{x,i}, \zeta_{y,i})$ and the location of the target is $\boldsymbol{z} = (x, y)$. For notational convenience, we rewrite the node position in polar coordinates (r_i, θ_i) where the origin is the target location. Then, the new coordinates are related to the Cartesian coordinates via

$$r_i^2 = (\zeta_{x,i} - x)^2 + (\zeta_{y,i} - y)^2, \ \tan\theta_i = \frac{\zeta_{y,i} - y}{\zeta_{x,i} - x}. \quad (1)$$

Let the ith element of an $N \times 1$ vector $\mathbf{t}$ represent an index corresponding to the type of the ith sensor so that $t_i \in \{1, \ldots, T\}$. The purpose of the sensors is to estimate the $2D$ target location $\boldsymbol{z} \in \Re^2$ of the target within $\mathcal{A}$. To achieve localization, each sensor type can provide an incomplete inference of the target position (range or bearing, but not both). Each sensor type is also characterized by a number of parameters including measurement error, sensor reliability, FOV, sensing range, and mobility as detailed in Section 4. Let Θ and $\mathcal{R}$ represent the modality sets associated to sensors that collect bearing and range measurements so that $\Theta \cup \mathcal{R} = \{1, \ldots, T\}$. Then, the ith node collects a bearing/range estimate if $t_i \in \Theta/\mathcal{R}$. To conserve energy, only a set of q sensors are activated to share their measurements to localize the target.

For simplicity, the sensors are indexed in ascending distance to the origin (i.e., target) $r_1 \leq r_2 \leq \ldots \leq r_N$. After deployment, the density for each sensor type-t, denoted as λ_t, is given by $\lambda_t = \frac{n_t}{A}$, where n_t is the total number of type-t sensors within a deployment area. The total number of sensors is denoted by $N = \sum_{t=1}^{T} n_t$. Moreover, each sensor's orientation ϕ_t is a uniform random variable on $[0, 2\pi)$.

It is known that the random deployment assumption can be well approximated by a Poison point process (PPP), and the joint distribution of the target distances for the first $k \ll N$ nodes is as follows [19]:

$$p(r_1, \ldots, r_k) = \left(\prod_{i=1}^{k} (2\pi\lambda r_i) \right) e^{-\pi\lambda r_k^2}, \quad (2)$$

for $0 \leq r_1 \leq r_2 \leq \ldots \leq r_k$. The marginal distributions for the distances follow scaled Chi distributions

$$p(r_i) = \frac{2}{\Gamma(i)} (\pi\lambda)^i r_i^{2i-1} e^{-\pi\lambda r_i^2} u(r_i). \quad (3)$$

In [13], we show that for nodes randomly distributed over a circular region, the histogram of the ordered distances to the region center follow (3) closely. The overall joint distribution of the coordinates for the k closest nodes can be written as

$$p(r_1, \theta_1, \ldots, r_k, \theta_k) = \lambda^k \left(\prod_{i=1}^{k} r_i \right) e^{-\pi\lambda r_k^2}, \quad (4)$$

since θ_i is *i.i.d.* and uniformly distributed.

3 The Design Problem

The objective of this design problem is to determine the vector $\boldsymbol{n}$ for deployment, which simultaneously satisfies multiple objectives and constraints such as utility (U), d-connectivity (C), v-coverage (V), network reliability B, and total resource \$. As detailed is Section 4, each sensor type has an effective sensing coverage radius R_t and an associated purchase cost c_t. The objectives and constraints are further explained below, followed by a mathematical definition of the design problem.

3.1 Utility

The utility function is defined as the reciprocal of the expected position MSE over all possible node locations:

$$U = \frac{1}{\text{stat}_{\boldsymbol{\zeta}} \left[\text{trace}\{\boldsymbol{F}_{\boldsymbol{z}}^{-1}\} \right]}, \quad (5)$$

where $\boldsymbol{F}$ is the Fisher information matrix derived in Section 4, and $\text{stat}_{\boldsymbol{\zeta}}\{\cdot\}$ is a statistic over the ensemble of possible node positions $\boldsymbol{\zeta}$ (in polar coordinates) that satisfies the following scaling property,

$$\text{stat}\{w\epsilon\} = w\text{stat}\{\epsilon\}, \quad (6)$$

where w is an arbitrary deterministic weight. Mean and median values are examples of such statistics. In the rest of the

paper, we refer to such statistics as typical values. In Section 5, we show that when only a constant number of sensors that minimize the localization error are activated, maximization of U in (5) w.r.t. the design variables is equivalent to the maximization of a weighted sum of the population of each sensor type:

$$\mathfrak{U} = \sum_{t=1}^{T} f_t n_t, \tag{7}$$

where f_t is a function of the sensor characteristics, such as the measurement noise σ_t, field of view α_t, reliability β_t, and sensor mobility μ_t.

3.2 Connectivity and Lifetime

In graph theory terms, a network is d-connected (with connectivity degree $C = d$) if, for any given pair of sensors, there exists at least d mutually independent paths connecting them [5]. Each sensor usually has a fixed transmission range r_{tran}, which is significantly smaller than the dimensions of $\mathcal{A}$. A communications link can be created between two sensors only if their physical distance is less than their transmission range. Hence, given transmission range r_{tran}, the probability of creating links between sensors increase as the number of sensors in the field increases.

Under the random deployment assumption, it is possible to show that the probability that each sensor has at least d-neighbors within the transmission range r_{tran} (node degree $D = d$) on a toroidal surface is given by the following [3]:

$$P(D \geq d|\boldsymbol{n}, \boldsymbol{\zeta}) \propto e^{N \log\left(1 - \sum_{k=0}^{d-1} \frac{\left(\pi\lambda r_{\text{tran}}^2\right)^k}{k!} \exp\left(-\pi\lambda r_{\text{tran}}^2\right)\right)}. \tag{8}$$

It is shown in [20] that in a graph, as the number of vertices increase, the node degree D converges to the connectivity degree C with probability one. In this paper, we approximate the connectivity of the sensor network by (8). In general, the connectivity probability should be simulated for the specific geometry of $\mathcal{A}$ (e.g., see [3] for simulations on square $\mathcal{A}$). It is important to note that the connectivity probability monotonically increases as a function of N. Hence, to maximize the connectivity probability (p_C) at any given degree, the total number of sensors N in the sensor network must be maximized.

Impacts of Connectivity on Power: Network connectivity can always be increased by increasing the sensor transmission range r_{tran}. However, the choice of r_{tran} also affects the lifetime (L) of the sensor network.[1] A sensor consumes power for ($\boldsymbol{\mathcal{A}}$) transmitting data, ($\boldsymbol{\mathcal{B}}$) receiving data, ($\boldsymbol{\mathcal{C}}$) sensing, ($\boldsymbol{\mathcal{D}}$) aggregating/fusing information, ($\boldsymbol{\mathcal{E}}$) idling, and ($\boldsymbol{\mathcal{F}}$) coping with radio interference/communications overhead/etc. [4, 8, 9, 24]. The sensor transmission range r_{tran} directly affects $\boldsymbol{\mathcal{A}}$ and indirectly affects $\boldsymbol{\mathcal{F}}$.

[1]The lifetime can be defined in various ways such as the time to first node failure due to battery depletion or the time to appearance of the first connectivity brake-down.

The explicit dependence of the sensor network lifetime on r_{tran} is beyond the scope of this paper. In [7], we explain that for a given transmission range that allows high connectivity, the lifetime of the sensor network linearly increases with the total number of sensors in the network as the total energy of the network is linearly increased (assuming efficient communication protocols that can minimize losses). Since the connectivity can be preserved with smaller transmission ranges as the number of sensors is increased, the actual lifetime of the sensor network grows faster than the growth obtained by increasing N while keeping r_{tran} fixed. Hence, when $p_C = 1 - \epsilon$ ($\epsilon \ll 1$), we assume that the network lifetime has approximately the following form:

$$L \propto N^{\delta}, \tag{9}$$

where $\delta > 0$ depends on the communication schemes and the propagation loss factor, and the proportionality is independent of r_{tran}. This form can also be motivated by the idealized case where the sensor batteries are depleted only by the r^p-propagation loss ($p \geq 4$): if p_C is high, then L can be shown to have the form in (9) (see [7]).

3.3 Coverage

The coverage (V) problem in sensor networks aims to quantify how well $\mathcal{A}$ is monitored. The coverage problem has been extensively studied in the literature, see Sect. 2 in [15] for a survey. Given the random deployment assumption, one can determine the number of sensors so that any given point in $\mathcal{A}$ is sensed by at least k-sensors with a given probability (k-coverage). For the sensor network design, the k-coverage probability is quite complicated as each sensor can have a heterogeneous sensing range R_t.

In [1], a Poisson approximation is given for the k-coverage probability for randomly deployed sensor networks with heterogeneous sensing ranges ($\kappa_t \triangleq \pi {R_t}^2/A$):

$$P(V \geq k|\boldsymbol{n}, \boldsymbol{\zeta}) = \sum_{l \geq k} \frac{\upsilon^l e^{-\upsilon}}{l!}, \text{ where } \upsilon = \sum_{t=1}^{T} \kappa_t n_t. \tag{10}$$

Note that the coverage probability is a monotonically increasing function of υ. To increase k-coverage probability to a desired level p_V, the average sensing area ($\upsilon \times A$ in (10)) must be maximized.

3.4 Reliability

In the context of sensors networks, reliability can imply sensing reliability and communications reliability. Communications reliability, which, e.g., relates to data loss corresponding to the packet drops in the communications channel, is beyond the scope of this paper. Instead, we focus on the sensing reliability where we assume that each sensor type-t has a constant reliability probability β_t, with which the sensor provides an observation to the network. In Section 5, we model the effects of sensor reliabilities on the localization performance of the whole network. However,

in the end, we also need to quantify how reliable the localization utility is based on the reliability of the sensors.

It is possible to show that under independence assumption of the sensor reliabilities, the average number of reliable sensors at any given time can be determined using the Binomial distribution: $\sum_{t=1}^{T} \beta_t n_t$. Hence, the fraction of the reliable sensors to the total number of sensors is a good metric to quantify the average sensing reliability of the sensor network, which is defined as

$$B = \frac{1}{N} \sum_{t=1}^{T} \beta_t n_t \tag{11}$$

For robustness, a critical number of sensors must be able to sense otherwise the network may not detect the target. A threshold b can be formulated as a linear constraint ($B \geq b$) which is handled in our solution.

3.5 The Pareto Optimization Problem

For the sensor network design, we consider the following optimization problem:

Design Problem: $[\boldsymbol{n}^*, r^*_{\text{tran}}] = \arg\max_{[\boldsymbol{n}, r_{\text{tran}}]} [U, L, V]$, subject to $p_C \geq p^*_C$, $p_V \geq p^*_V$, $B \geq b$, sensor management constraints (Sect. 5), and $\boldsymbol{n}^* \in \boldsymbol{\mathcal{N}} = \{\boldsymbol{n} | n_m \geq 0, \forall m; \boldsymbol{c}'\boldsymbol{n} \leq \$\}$.

This is a multi-criteria problem over the simplex $\boldsymbol{\mathcal{N}}$ with three competing objectives: a utility objective that spends resources on utility maximizing sensors, a lifetime objective that spends resources to maximize the number of sensors regardless of their utility, and a coverage objective that tries to increase the number of sensors covering a certain point regardless of their utility. The simplex is defined by design vector $\boldsymbol{n}$, the cost vector $\boldsymbol{c}$, and the budget \$, which denote the cost of each sensor type and the total resource available for creating the sensor network. Multi-criteria objective problems are typically addressed using Pareto optimality. In general, enumeration of all possible parameter choices that satisfy the constraints is required to explore the Pareto trade-off surface of U, L, and V [6]. However, in the end, some preference must be made to choose an operating point. In the appendix, we provide a integer programming solution to determine the Pareto surface. In [7], we discuss how continuous relaxations can be used to improve the efficiency of the solution and elaborate how to determine r_{tran}.

4 Sensor Characteristics

4.1 Observation Characteristics

We consider two types of sensor models that observe the bearing θ or the range r of targets. The range and bearing of a target at position $\boldsymbol{z} = (x, y)$ is defined in (1). Each sensor makes an observation o_i ($i = 1, \ldots, N$). The sensor either collects a bearing or range measurement depending on its sensor type t. If $t \in \Theta$ then the observation follows an additive white Gaussian noise model:

$$o_i = \theta_i + \sigma_t(r_i)\mathcal{N}(0, 1). \tag{12}$$

In other words, the bearings sensor measure a noisy version of the true bearing. If $t \in \mathcal{R}$, the observations of the range sensors follow a multiplicative noise model:

$$o_i = r_i e^{\sigma_t(r_i)\mathcal{N}(0,1)}. \tag{13}$$

The noise of the range measurement grows in concert with the actual range. In fact, the multiplicative model given by (13) states that the observations follow a log-normal distribution. Such a measurement model is appropriate for video camera system and other sensor types. It is assumed that the sensors are spaced sufficiently far from each other so that their measurements are independent. Overall, the measurement modes lead to the following distribution of the measurements made by the active sensor set $\mathcal{N}_q$, which has q sensors selected by a management strategy (see Sect. 5):

$$P(O|\boldsymbol{z}) = \prod_{i:t_i \in \Theta \& i \in \mathcal{N}_q} \frac{1}{\sqrt{2\pi\sigma^2_{t(i)}(r_i)}} \exp\left\{ -\frac{(o_i - \theta_i)^2}{2\sigma^2_{t(i)}(r_i)} \right\} \times$$
$$\prod_{i:t_i \in \mathcal{R} \& i \in \mathcal{N}_q} \frac{1}{o_i\sqrt{2\pi\sigma^2_{t(i)}(r_i)}} \exp\left\{ -\frac{\left(\log(o_i) - \log(r_i)\right)^2}{2\sigma^2_{t(i)}(r_i)} \right\}. \tag{14}$$

For both the bearing and range measurement models, we consider the fact that the measurement error σ_t^2 can grow with increasing range: $\sigma_t^2(r) = \sigma^2_{\text{rf},t} r^a$, where $\sigma_{\text{rf},t}$ is the error associated to a reference distance of $r = 1$. One would expect that the measurement error grows with distance due to an r^p propagation loss in the signal to noise ratio, which occurs in free space. In fact, the analysis of DOA estimation of arrays indicates that $a = 2$ near the target [2, 7]. However, in the real world the signal is propagating though a non-uniform medium. For acoustical arrays, the atmospheric effects of propagation to the Cramer-Rao lower bound (CRLB) of bearing estimation has been studied in [22]. It is shown that for a simple two element array, the performance of bearing estimation is constant within a critical range to the target because the performance is limited by the atmospheric turbulence (not measurement noise). Numerical calculations using tools developed in [23] reveals the same observation for more complex arrays. Analysis of calibration errors can also show that within a critical range, the performance of any array (not necessarily an acoustic array) is constant within a critical range. Therefore, for some cases, it is also reasonable to assume that within the sensing range of the sensor's modality, the measurement error may be constant $a = 0$. We develop the analysis for general values of a, but place close attention to the $a = 0$ case.

4.2 Localization Performance

Once deployed, the sensors are able to use the knowledge of their location ($\boldsymbol{\zeta}_i$ for $i = 1, \ldots, N$) to estimate the target's location. However, the target is localized using the range and bearing measurements from only the active set of sensors $\mathcal{N}_q$ at any given time. Using the problem geometry and the sensor measurement models, the localization

information can be quantified using the Fisher information matrix $\boldsymbol{F}$, which is defined as follows [16]:

$$\boldsymbol{F}_{\boldsymbol{z}} = \int p(O|\boldsymbol{z}) \left[\frac{\partial \log p(O|\boldsymbol{z})}{\partial \boldsymbol{z}}\right] \left[\frac{\partial \log p(O|\boldsymbol{z})}{\partial \boldsymbol{z}}\right]^T dO, \quad (15)$$

where $p(O|\boldsymbol{z})$ is given by (14). It has been demonstrated that a network of bearing sensors implementing the maximum likelihood (ML) position estimator can achieve the CRLB [14]. Hence, it is reasonable to approximate the MSE estimate over all possible measurement realizations as

$$\epsilon(\mathcal{N}_q, \mathbf{r}, \boldsymbol{\theta}) = \text{trace}\{\boldsymbol{F}_{\boldsymbol{z}}^{-1}\}. \quad (16)$$

Given (14) and (15), it can be shown that

$$\boldsymbol{F}_{\boldsymbol{z}} = \sum_{i \in \Theta \cap \mathcal{N}_q} \boldsymbol{F}_{\theta,i} + \sum_{i \in \mathcal{R} \cap \mathcal{N}_q} \boldsymbol{F}_{r,i} + \sum_{i \in \mathcal{N}_q} \boldsymbol{F}_{\sigma,i}, \text{ where } \quad (17)$$

$$\boldsymbol{F}_{\theta,i} = \frac{1}{\sigma_{\text{rf},t_i}^2 r_i^{a+2}} \boldsymbol{M}(\theta_i), \quad \boldsymbol{F}_{r,i} = \frac{1}{\sigma_{\text{rf},t_i}^2 r_i^{a+2}} \boldsymbol{M}\left(\theta_i - \frac{\pi}{2}\right),$$

$$\boldsymbol{F}_{\sigma,i} = \frac{a^2}{2r_i^2} \boldsymbol{M}(\theta_i), \quad \boldsymbol{M}(\theta_i) = \begin{bmatrix} \sin^2\theta_i & -\frac{1}{2}\sin 2\theta_i \\ -\frac{1}{2}\sin 2\theta_i & \cos^2\theta_i \end{bmatrix}.$$

The matrix $\boldsymbol{F}_{r,i}$ (or $\boldsymbol{F}_{\theta,i}$) represents the information available from the range (or bearing) measurement of the ith sensor. The matrix $\boldsymbol{F}_{\sigma,i}$ represents the extra information gained when exploiting the fact that the measurement error is a function of range. For $a = 0$, the measurement error is independent of range, and the $\boldsymbol{F}_{\sigma,i}$ term disappears. When $a \neq 0$ the $\boldsymbol{F}_{\sigma,i}$ matrix is dominated by the $\boldsymbol{F}_{r,i}$ or $\boldsymbol{F}_{\theta,i}$ matrix as r_i approaches zero. In fact, it is reasonable to assume that the $\boldsymbol{F}_{\sigma,i}$ matrix is insignificant when r_i is within the sensing radius as further discussed in Section 4.1.

4.3 Other Sensor Characteristics

4.3.1 Field-of-View

Most sensors do not exhibit an omnidirectional FOV, and a sensor can only make a measurement of a target that is within its FOV. In this paper, we only consider the azimuthal FOV, which is the horizontal angular extent around the line of sight for which the sensor can make measurements. We use α_t to represent the normalized FOV for type-t sensors, i.e., the angular extent of the FOV in radians divided by 2π radians. When $\alpha_t = 1$, the sensor type is omnidirectional, e.g., microphones. Otherwise, $\alpha_t < 1$.

4.3.2 Sensing Range

Sensors can detect a target and make range or bearing measurements as long as the signal to noise ratio (SNR) is sufficiently high. Clearly, the SNR degrades as the range between the sensor and target increases. Many sensors exhibit consistent performance until the SNR fall below a critical value. When the SNR is above the critical value, the measurement error σ_t is fairly constant. On the other hand, when the target range is far enough so that the SNR falls below the critical value, then σ_t blows up and the detection probability goes to zero. Data in [14] indicates that $\sigma_t \approx 3 - 5^\circ$ when the range is less than 500 meters for the tested acoustic arrays. We denote R_t as the sensing range of the type-t sensors. Such sensors can only make a measurement if $r < R_t$.

4.3.3 Reliability

The reliability of a sensor is given by the parameter $0 \leq \beta_t \leq 1$. This parameter represents the probability that a sensor can make a measurement and communicate it to its neighbors. This parameter models both the ability of the sensor to make a measurement and the ability of the radio on the sensor to transport the measurement to other sensors. When $\beta_t = 1$, the sensor is completely reliable.

4.3.4 Cost

Each sensor type has a monetary cost. Given a fixed financial budget, one can clearly afford to procure and deploy more cheaper sensors than more expensive sensors. The unit cost of type-t sensors is labeled as c_t.

4.3.5 Mobility

The mobility parameter $\mu_t \in \{0, 1\}$ is a binary value that states whether or not the sensor can move. When $\mu_t = 1$ the sensor type is mobile, and when $\mu_t = 0$, the sensor type is stationary. In this work, we consider mobile sensors that operate in a random search mode. Both the stationary and mobile sensors are initially distributed uniformly over the surveillance region. As a result, the distribution of the sensors within the surveillance region are well modeled as a PPP. The mobile sensors follow a random walk so that the location of the sensors from one snapshot to the next continue to follow the PPP model. The average speed of the sensors is large enough so that the configuration of mobile sensors from one snapshot to the next can be viewed as statistically independent of each other.

5 Effects of Sensor Management

The statistics of the network geometry and the FIM allow for characterization of the typical values of the localization performance of the sensor network. This section provides a theory to explain the typical localization performance when employing sensor management. First, it is demonstrated that the network design strategy is agnostic to the measurement type (range or bearing). Then, the typical performance is derived when the network incorporates a node selection strategy that activates q nodes per snapshot in order to conserve energy. Finally, the typical performance is extended to include mobile nodes that enhance the spatial diversity of the network.

5.1 Duality of Range and Bearing Sensors

Range and bearing sensors provide different measurements that both can be used to localize a target. Once the nodes are emplaced and the network is operating, the selection of active sensors **does** depend on the measurement

type. Each measurement type provides good localization in one direction and infinitely poor localization in the other. For instance, a bearing sensor provides good localization in azimuth but no localization in range. The opposite is true for range sensors. As a result, for two bearing sensors to provide good localization of a target, they should be located so that their line of sights to the target are nearly perpendicular. On the other hand, if the line of sights are nearly parallel, there will be no localization in range. A similar situation occurs for two range sensors. However, given one range and one bearing sensors, the two sensors should be located so that their line of sights are parallel w.r.t the target. Once the network is operating, the sensor manager must understand which type of measurement (range or bearing) the node can collect.

For the uniformly random deployment of nodes, two sensors are equally likely to have nearly perpendicular line of sights to the target (at an arbitrary point) as they are to have nearly parallel line of sights. In fact, when considering which nodes to deploy, the measurement type does not matter. For any random configuration, any bearing node could be replaced by a range node in a different location to form another equally likely configuration that provides equivalent localization to a specific point. In other words, when considering random node deployments, the range and bearing sensors exhibit a duality.

Let us consider a modality t that consists of n_t bearing sensors with $\sigma_t(r) = \sigma_{\text{rf},t} r^{a/2}$. Furthermore the FOV, reliability, sensing range, and mobility are α_t, β_t, ρ_t, and μ_t, respectively. A random configuration of the sensors can be given by $\boldsymbol{\zeta}_i = (r_i, \theta_i)$ for $i = 1, \ldots, n_t$. The FIM associated to each node is given by $\boldsymbol{F}_{\theta,i}$ in (17). Let us rotate the configuration $\pi/2$ about the target location and exchange the bearing sensors for range sensors with the same values for $\sigma_t(r)$, α_t, β_t, ρ_t, and μ_t. Now, the geometry of the sensors is given by $\boldsymbol{\zeta}_i = (r_i, \theta_i + \frac{\pi}{2})$. The FIM associated to the range sensors is given by $\boldsymbol{F}_{r,i}$ in (17) where $\theta_i + \frac{\pi}{2}$ is substituted for θ_i. After this substitution, the FIM contribution for each range sensor is equivalent to the corresponding bearing sensor's FIM contribution $\boldsymbol{F}_{r,i}$ before the rotation. As a result, the MSE given by (16) for the target localization is the same for these two configurations. Because the polar angles are uniformly distributed over $[0, 2\pi)$, the original configuration is as equally likely to be realized as the rotated configuration. As a result, the MSE error distributions due to random configurations of range or bearing sensors will be equivalent. As a corollary, the typical values of a network design does not change if the bearing modalities are exchanged for range modalities of equivalent density, measurement error, FOV, reliability and mobility. Likewise, the same is true if the range modalities are exchanged for bearing modalities.

The duality between the bearing and range sensors is exact when the measurement errors are constant over range, i.e., $a = 0$. When $a \neq 0$, the duality is approximate because it ignores the $\boldsymbol{F}_{\sigma,i}$ contribution. As stated earlier, this matrix can be ignored when the node is within the sensing range of the target.

Finally, the FIM does not account for measurement ambiguities. It only considers the spread of possible values around the modes of the likelihood. In two dimensions, it takes three range (or bearing) sensors to localize a target without ambiguity. Therefore, for pure target localization without incorporating measurements from prior snapshots, the sensor manager must set $q \geq 3$ for the duality to be meaningful. In practice, a track filter provides a predicted target location that removes the ambiguity and allows the duality to exist for $q < 3$.

5.2 A Sensor Management Strategy based on Selecting q-Sensors

A reasonable sensor management approach searches for the best q sensors to actively collect and share measurements over one snapshot. The management strategy attempts to determine an active set $\mathcal{N}_q$ of cardinality q (i.e., $|\mathcal{N}_q| = q$) that minimizes the expected MSE given by (16) over all possible sensors. When the sensor manager is operating, it does have knowledge of the sensor locations. However, it does not have knowledge of the exact target location to place the origin of the coordinate system to determine the values $\boldsymbol{\zeta}_i$ used in (16)–(17). In practice, the sensor management centers the coordinate system around an estimate of the predicted target location from a track filter.

One sensor management approach simply selects the closest sensors after the distances are normalized by the measurement error σ. Let the normalized distance be

$$\tilde{r}_i = \sigma_{\text{rf},t_i}^{\frac{2}{a+2}} r_i, \tag{18}$$

and let $m(i)$ be the mapping $m : \{1, \ldots, N_s\} \rightarrow \{1, \ldots, N_s\}$ that rank orders the normalized distances, i.e.,

$$\tilde{r}_{m(1)} \leq \tilde{r}_{m(2)} \leq \ldots \leq \tilde{r}_{m(N_s)}. \tag{19}$$

The closest approach simply selects the q closest nodes

$$\mathcal{N}_q(\mathbf{r}, \mathbf{t}) = \{m(i) : i = 1, \ldots, q\}. \tag{20}$$

The active set is a function of the node ranges and modalities. The closest approach ignores the bearing information and only focuses on reducing the trace of the FIM in (17). As shown in [12], as q grows, the closest approach is effective in reducing the MSE.

The global node selection method accounts for the complete target-node geometry. It selects the active set to minimize the MSE, i.e.,

$$\mathcal{N}_q(\mathbf{r}, \boldsymbol{\theta}, \mathbf{t}) = \underset{\mathcal{N}:|\mathcal{N}|=q}{\operatorname{argmin}} \epsilon(\mathcal{N}), \tag{21}$$

where the complete expression for the MSE is given by (16)-(17). The GNS method is a function of the complete node-target geometry as well as the modality of each node. Implementation of (21) via exhaustive search can be very cumbersome due to the combinatorial explosion as N becomes large. A suboptimal Greedy search is provided in [12], and it is demonstrated in [12] that the search determines an active set whose MSE is close to the optimal. It should also be noted that the active set selected by the Greedy search is still a function of the complete target/node geometry as well as the modality of each node.

The MSE as expressed in (16)-(17) is explicitly a function of the geometry and modality of the network configuration as well as the active set selected by the sensor management strategy. Any sensor management strategy can be viewed as a function whose input is the geometry and modality of the network configuration, i.e., $\mathcal{N}(\mathbf{r}, \boldsymbol{\theta}, \mathbf{t})$. The output is a set of active sensors. For the closest and GNS approaches, this function is given by (20) and (21), respectively. As a result, the MSE is a function that only depends on the geometry and modality of the network. Furthermore, the distribution describing the closest k sensors is given by (4). Given that $q \ll k$, it is expected that all sensors selected by the closest and GNS approaches are encompassed by the k closest nodes. Then, one can theoretically determine the distribution of the MSE resulting over all network configurations. However, the development of a closed form expression of the distribution is difficult (if not impossible). One could theoretically calculate the mean MSE by calculating the indefinite integral of (16) multiplied by (4). Again, this integral is not trivial, and for the closest approach with $q = 2$ and $a = 0$, we have shown that it is divergent [13]. Because of this divergence, we consider looking at the broader class of typical values.

While closed form expressions of typical values for the MSE might be elusive, one can compute typical statistics using Monte Carlo realizations for one special case of each sensor management approach with a given value of q and known measurement decay a. The special case is a homogenous network where $\lambda = 1$, and the sensor characteristics are $\sigma = 1$, $\alpha = 1$, $\beta = 1$, and $\mu = 0$. The main result of the paper is that an expression for the localization performance of a general heterogeneous sensor network is simply scaled by a constant determined by a typical value derived from Monte Carlo realizations of the special case. The remainder of the section is devoted to deriving this expression. First, we show how to derive the performance of a general homogeneous network from the special case. Then, results are extended for the heterogeneous network.

Characterization of Homogeneous Networks The derivation starts with a homogeneous network consisting only of sensors of type-t so that $\lambda = \lambda_t$ and $\sigma_{t_i}(r_i) = \sigma_t(r_i)$. Furthermore, the other sensor parameters such as the FOV and reliability are constant over the node index i. While the node density is λ_t, not every node will be functional. Due to the random deployment of the sensors, the orientation of the sensor is a random value whose distribution is uniform over $[0, 2\pi)$. Because the normalized FOV is α_t, each node has an α_t probability of having line of sight to an arbitrary point. Therefore, the probability that a node can make a useful measurement is α_t. Furthermore, the node is reliable with a probability of β_t. Overall, the probability that the node is able to make a useful measurement and communicate it to other sensors in the network is $\alpha_t\beta_t$. It is well known that when a 2-D PPP of density λ_t provides useful nodes with a probability of $\alpha_t\beta_t$, the distribution of effective sensors is also a 2-D PPP with a density of $\lambda_{\text{eff},t} = \alpha_t\beta_t\lambda_t$ [21]. The joint distribution of the location of the effective sensors is given by (4) where $\lambda_{\text{eff},t}$ replaces λ_t. The effective sensors can be viewed as having omnidirectional FOV ($\alpha = 1$) and complete reliability ($\beta = 1$).

For the homogeneous network, the normalized distance is simply a scaled version of the actual distance where the scale factor is $\sigma_{\text{rf},t}^{2/(a+2)}$ (see (18)). The joint distribution of the geometry with respect to the normalized distances can be obtained from (4) via a change of variable so that

$$p(\tilde{r}_1, \theta_1, \ldots, \tilde{r}_k, \theta_k) = \tilde{\lambda}^k \left(\prod_{i=1}^{k} \tilde{r}_i \right) e^{-\pi\tilde{\lambda}\tilde{r}_k^2}, \tag{22}$$

where

$$\tilde{\lambda} = \frac{\lambda_{\text{eff}}}{\sigma_t^{4/(a+2)}} = \frac{\alpha_t\beta_t}{\sigma_t^{4/(a+2)}}\lambda_t. \tag{23}$$

In other words, the distribution of normalized node locations $(\tilde{r}_i, \theta_i)$ can be viewed as being drawn from a 2-D PPP with rate $\tilde{\lambda}$. Furthermore, the normalized configuration does not depend on the measurement accuracy $\sigma_{\text{rf},t}$ so that the MSE expression given by (16) is independent of sensor type when considering the normalized density $\tilde{\lambda}$.

By performing a change of variables with $\bar{r}_i = \sqrt{\tilde{\lambda}}\tilde{r}_i$, the joint distribution of $(\bar{r}_i, \theta_i)$ exhibits a unit density,

$$f(\bar{r}_1, \theta_1, \ldots, \bar{r}_k, \theta_k) = \left(\prod_{i=1}^{k} \bar{r}_i \right) e^{-\pi\bar{r}_k^2}, \tag{24}$$

and the location of sensors given by $(\bar{r}_i, \theta_i)$ are drawn from a 2-D PPP of unit density. In other words, the sensor locations represent the special case of unit density, measurement error, FOV, and reliability. The overall MSE is a scaled version of the MSE for the reference 2-D PPP, i.e.,

$$\epsilon(\mathcal{N}_q, \mathbf{r}, \boldsymbol{\theta}) = \frac{1}{\tilde{\lambda}^{(a+2)/2}} \bar{\epsilon}(\mathcal{N}_q, \bar{\mathbf{r}}, \boldsymbol{\theta}) \tag{25}$$

where $\bar{\epsilon}(\mathcal{N}_q)$ is the MSE for the special case of unit error ($\sigma_{\text{rf},i} = 1$) i.e.,

$$\bar{\epsilon}(\mathcal{N}_q, \bar{\mathbf{r}}, \boldsymbol{\theta}) = \text{trace}\left\{ \left(\sum_{i \in \mathcal{N}_q} \frac{1}{\bar{r}_i^{a+2}} \boldsymbol{M}(\theta_i) \right)^{-1} \right\}. \tag{26}$$

The distribution of $\bar{\epsilon}(\mathcal{N}_q, \bar{\mathbf{r}}, \boldsymbol{\theta})$ can be used to determine reference typical values for which the typical MSE values of other homogeneous networks can be calculated by exploiting (25) and the scaling property (6).

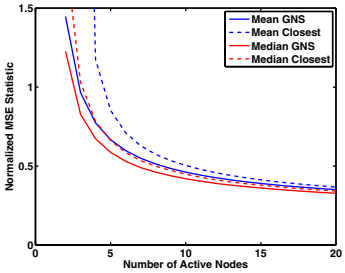

Figure 1. The MSE localization performance

The reference network helps avoid the calculation of a closed from expression for the distribution of the MSE of the arbitrary homogeneous network, which is difficult (if not impossible) to obtain. For the special case of the closest sensor selection method with $q = 2$, a closed form expression for the MSE distribution appears in [13]. For other cases, where the distribution is elusive, one can calculate typical values associated to the distribution from Monte Carlo realizations of random sensor network configurations. The typical values are functions of the sensor management strategy including the value of q. Therefore, each sensor management strategy requires another Monte Carlo simulation. Let $\bar{\varepsilon}^{\text{stat}}_{s,q}$ represent the reference MSE for typical value stat $\in \{\text{mean}, \text{median}\}$ and sensor management method s (s="c" or s="g"for the closest and GNS approaches, respectively), when q sensors are active per snapshot. Given the sensor management method, the typical MSE for the general homogeneous sensor network is

$$\text{stat}\{\epsilon\} = \frac{\bar{\varepsilon}^{\text{stat}}_{s,q}}{\left(\frac{\alpha_t \beta_t}{\sigma^{4/(2+a)}_{\text{rf},t}} \lambda_t\right)^{(a+2)/2}}. \tag{27}$$

Figure 1 plots the values of $\bar{\varepsilon}^{\text{stat}}_{s,q}$ as a function of q for various sensor management strategies and typical values when $a = 0$. These scale constants were obtained by generating 10000 random configurations of 1000 sensors uniformly distributed over a circular region of radius $R \approx 17.84$m so that the density is $\lambda = 1$. Because of (25), the trends seen in the figure extend to any heterogeneous sensor network. The figure shows that the mean MSE always exceed the corresponding median MSE. Furthermore, GNS leads to a lower MSE than the closest strategy for the same k. However, the gap between the GNS and closest approaches decreases as q becomes large, and the implementation of the GNS is only necessary for small q.

Characterization of Heterogeneous Networks The transition from a homogeneous network to a heterogeneous network is now relatively straightforward when considering the normalized positions of the sensors $(\tilde{r}_i, \theta_i)$ in the sensor network. The set of sensors representing sensor type-t represent a PPP of effective rate $\tilde{\lambda}_t = \lambda_{\text{eff},t}/\sigma_t^{4/\alpha}$. The aggregation of all sensor types actually means that the normalized positions are drawn from a PPP with a rate that is the sum of the aggregates, [21]

$$\tilde{\lambda} = \sum_{t=1}^{T} \tilde{\lambda}_t. \tag{28}$$

Then because of (24) and (25), the typical MSE of the heterogeneous network is

$$\text{stat}\{\epsilon\} = \frac{\bar{\varepsilon}^{\text{stat}}_{s,q}}{\left(\sum_{t=1}^{T} \frac{\alpha_t \beta_t}{\sigma^{4/(2+a)}_{\text{rf},t}} \lambda_t\right)^{(a+2)/2}}. \tag{29}$$

Equation (29) is one of the main results of this paper. By (5) and the fact that $\lambda_t = n_t/A$, the utility (5) of the network design is

$$U = \frac{1}{A^{(a+2)/2} \bar{\varepsilon}^{\text{stat}}_{s,n}} \left(\sum_{t=1}^{T} \frac{\alpha_t \beta_t}{\sigma^{4/(2+a)}_{\text{rf},t}} n_t\right)^{(a+2)/2}. \tag{30}$$

No matter the value of a, the sensor management strategy, or the chosen typical value, the maximization of the utility in (30) is equivalent to the maximization of

$$\mathfrak{U} = \sum_{t=1}^{N} f_t n_t, \text{ where} \tag{31}$$

$$f_t = \frac{\alpha_t \beta_t}{\sigma^{4/(2+a)}_{\text{rf},t}}. \tag{32}$$

Most importantly, the calculation of the localization utility given by (31)-(32) does not depend on the chosen typical value or how the implemented sensor management strategy chooses the q-active sensors.

5.3 Mobility

The utility given by (31)-(32) only considers stationary sensors, i.e., $\mu_t = 0$. When collecting measurements over multiple snapshots, mobile sensors can provide better spatial diversity to improve localization performance. As discussed earlier, this paper considers mobile sensors that follow a random walk. The velocity of these sensors is such that at each snapshot, they form a configuration that is statistically independent of the previous configuration. To simplify the analysis, the target is assumed to be moving slow enough that it can be considered stationary over N_o snapshots. This means that over the N_o snapshots, the covariance update of the track filter is simply the inverse of the sum of the FIMs over the N_o snapshots.

Let us first consider a network of stationary sensors. Each snapshot selects the same active set for a stationary

target. The aggregate FIM is simply $\boldsymbol{F_z}$ scaled by N_o, and the contribution of each node to the FIM is $\boldsymbol{F}_{\theta,i}$ in (17) scaled by N_o. Recall that due to the duality of range and bearing sensors, $\boldsymbol{F}_{\theta,i}$ and $\boldsymbol{F}_{r,i}$ are equivalent after averaging over the ensemble of configuration realizations. The value of N_o can be absorbed by the measurement error so that aggregating of N_o snapshots is equivalent to the ith node measurement error reducing to $\sigma_{\text{rf},t_i}/\sqrt{N_o}$. Overall, the weighting factor in the utility objective of (31) is now

$$f_t' = N_o^{2/(2+a)} f_t, \tag{33}$$

where f_t is given by (32).

When the sensors are mobile, the aggregate FIM is still the sum of N_o FIMs. However, each FIM associated to a snapshot is due to an independent random configuration. Each snapshot selects q sensors. Over the N_o snapshots, qN_o sensors are selected to be active. The aggregate of the N_o random configurations can be view as being drawn from a $2D$ PPP whose density is N_o times the effective density of the network. The localization utility of the network can be computed by interpreting that the sensor management applied over each snapshot to select q sensors is equivalent to sensor management applied over the aggregation of the N_o configurations to select qN_o sensors. As a result, the utility in (30) can be expressed as

$$U = \frac{1}{A^{(a+2)/2}\bar{\varepsilon}_{s,q}^{\text{stat}}} \left(\sum_{t=1}^{T} N_o \left(\frac{\bar{\varepsilon}_{s,q}^{\text{stat}}}{\bar{\varepsilon}_{s,qN_o}^{\text{stat}}} \right)^{\frac{2}{a+2}} f_t n_t \right)^{\frac{a+2}{2}}. \tag{34}$$

Overall, the weighting factor in the utility objective N_o snapshots is

$$f_t' = N_o \left(\frac{\bar{\varepsilon}_{s,q}^{\text{stat}}}{\bar{\varepsilon}_{s,qN_o}^{\text{stat}}} \right)^{\frac{2}{a+2}} f_t. \tag{35}$$

Actually, the localization utility formed by this interpretation is an upper bound because the "best" sensors selected over the aggregate configuration may not distribute uniformly over the N_o random configurations. In other words, the qN_o sensors formed by applying sensor management over each configuration separately can lead to a different set of sensors than applying the sensor management over the aggregate configuration. While the interpretation actually provides an upper bound on the utility, simulations indicate that the bound is tight (see Section 6).

When the network consists of a mixture of mobile and stationary sensors, it is not clear how to interpret the selection of the sensors over the aggregate. Without any theoretical justification, we simply use f_t' in (33) or (35) when the sensor node is stationary ($\mu_t = 0$) or mobile ($\mu_t = 1$), respectively. This approximation leads to the proper results when all sensors are stationary or mobile, and it provides an interpolation when the network is mixed.

The general expression for the typical value using sensors that integrate over N_o snapshots is now

$$\text{stat}\{\epsilon\} = \frac{\bar{\varepsilon}_{s,q}^{\text{stat}}}{\left(\sum_{t=1}^{T} \frac{N_o^{\frac{1-\mu_t}{1+a/2}} \left(N_o \left(\frac{\bar{\varepsilon}_{s,q}^{\text{stat}}}{\bar{\varepsilon}_{s,qN_o}^{\text{stat}}} \right)^{\frac{2}{2+a}} \right)^{\mu_t} \alpha_t \beta_t}{\sigma_t^{4/(2+a)}} \lambda_t \right)^{\frac{a+2}{2}}}. \tag{36}$$

When the measurement errors are not range dependent, i.e, $a = 0$, the utility of the stationary sensors grows linearly with N_o, and the utility of the mobile sensors grows faster than linear due to the ratio $\frac{\bar{\varepsilon}_{s,q}^{\text{stat}}}{\bar{\varepsilon}_{s,qN_o}^{\text{stat}}}$. Therefore, the advantage of mobile sensors over stationary ones becomes more pronounced as the value N_o becomes larger. Note that the limiting factor for N_o is the number of snapshots that it is reasonable to assume the target is stationary. The faster the target, the smaller the achievable N_o. When $a > 0$, the utility of the stationary nodes increases sublinearly with respect to N_o, and the utility of the mobile nodes still grows faster than linear. Overall, for a given q, the localization advantage of the mobile sensor over the stationary sensor become larger for larger values of a. Nevertheless, mobile sensors provide better localization than stationary ones when $N_o > 1$ for the $a = 0$ case.

6 Simulations

Localization Performance We provide Monte Carlo simulations to establish the correctness of the localization formulaes. In all simulations, the sensors have omnidirectional FOVs, i.e., $\alpha_{t_i} = 1$, and complete reliability $\beta_{t_i} = 1$ and we have $a = 0$. The results are either presented as root mean squared (RMS) position error, i.e., the square root of (36), or as the utility, i.e., the reciprocal of (36). For the Monte Carlo simulations, 1000 random realizations are created per each free parameter, and the RMS position error and the utility are calculated as the square root and reciprocal, respectively, of the typical MSE value over the 1000 realizations using various sensor management strategies with $q = 4$. Each realization of the sensor network configuration distributes the nodes via random uniform distribution over a circle of radius 100 meters, and the target location is the center of the circle.

We first demonstrate the ability to predict the localization accuracy for a heterogeneous network of stationary nodes, i.e., $\mu_{t_i} = 0$. The network consists of two types of bearing nodes: Type 1 provides a bearing error of $\sigma_1 = 5^\circ$ at a cost of $c_1 = 1$ unit, and Type 2 provides a bearing error of $\sigma_2 = 1^\circ$ at a cost of $c_2 = 5$ units. The budget is 1000 units.

Figure 2 plots the RMS position error for various network designs when using the two sensor management approaches discussed in Section 5. Clearly, the Monte Carlo simulations results matches the theoretical performance rather well. The curves indicate a monotonic trend between the homogeneous cases, which is due to the linearity of the utility. Despite the higher cost of the type-2 sensors, one

would incorporate only these sensors if localization is the only performance objective.

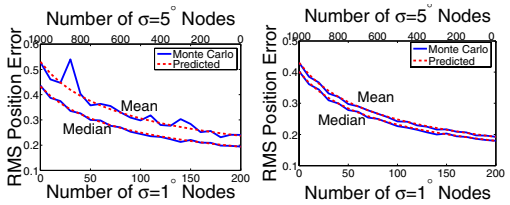

(a) Closest (b) GNS

Figure 2. Comparison of theory and Monte Carlo simulations

The next simulation investigates the processing gains when $N_o > 1$ for both stationary and mobile sensors. In these simulations, both sensor types achieve a measurement error of $\sigma_t = 5°$. Figures 3(a)-(b) plot the utility versus N_o for the closest and GNS sensor management approaches, respectively, and Figure 3(c) compares the sensor management approaches. In these plots, the typical value is the mean. The curves clearly demonstrate that the mobile nodes become more advantageous as N_o grows. The predicted performance is well matched to the simulated results for the "closest" node selection approach. The predicted utility for mobile nodes implementing GNS are larger than the simulated results. As stated earlier, the predicted utility for mobile sensors is an upper bound of the performance. Furthermore, for large N_o, the GNS performs worse than the closest approach for the mobile nodes as seen in Figure 3(c). Certainly, over one configuration, the GNS demonstrates better utility than the closest approach. However, GNS is myopic, and it can forgo potentially good nodes for a given snapshot due to a poor geometry without considering the aggregate node geometry over the integration time. On the other hand, the closest approach is able to reduce the trace of the FIM in (17) as it relies on spatial diversity of the moving nodes to ensure that the FIM determinant is large so that (16) can be small.

The third simulation assesses the performance of a mixed network of mobile and stationary sensors. The mobile nodes cost 5 units, the stationary nodes cost 1 unit, and the total budget is 1000 units. Beyond mobility, the two sensor types are identical. Both sensor types produce bearing estimates with $\sigma = 5°$. Figure 4 plots the RMS position error against possible network designs. For the closest approach, the predicted performance matches the simulations very well at the end points, i.e., homogeneous networks. For the median value, the match is still good for mixed networks. The mean value is slightly better than predicted by the interpolation used for mixed networks. For the GNS management approach, the predicted mean and median values are well matched to the simulations except as the network consists of exclusively mobile sensors. As in the previous simulation, the myopic strategy degrades the performance of GNS for mobile nodes more so than the closest approach, and the actual localization performance is slightly worse than predicted.

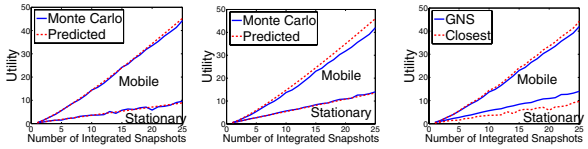

(a) Closest (b) GNS (c) Closest vs. GNS

Figure 3. Utility vs. N_o

Multi-Objective Pareto Frontier Using a synthetic example, we demonstrate the dynamic programming solutions of the design problem. We consider a toy example including $T = 6$ sensor types. The nodes are stationary and their sensor characteristics lead to an effective density (see (32)) of $f_t = t^2$. Furthermore, $c_t = 1 + t$, $\delta = 1.2$, $a = 2$, $\$ = 500$, $\boldsymbol{R} = [\,1,\ 2,\ 2,\ 2,\ 3,\ 3]$, and $\boldsymbol{\beta} = [\,0.95,\ 0.9,\ 0.8,\ 0.85,\ 0.7,\ 0.8]$. For ease of visualization, we simultaneously maximize only U, L, and V.

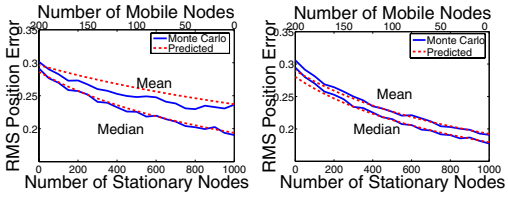

(a) Closest (b) GNS

Figure 4. Localization performance of a mixed network

Figure 5(a) shows the $3D$ Pareto frontier surface. In the solution, U is maximized at $n = 72$ where $\boldsymbol{n} = [\,0,\ 1,\ 0,\ 0,\ 0,\ 71]$ V is maximized at $n = 84$ where $\boldsymbol{n} = [\,1,\ 0,\ 0, 0,\ 83,\ 0]$. Figures 5(b) illustrates the constant average reliability B support contours of the $3D$ Pareto surface as a fourth dimension, which can be calculated using the dynamic programming solution. Figure 5(c) demonstrates the distribution of the resources (*top*) at a constant coverage V while trading lifetime L for utility U starting from maximum utility, (*middle*) at a constant lifetime while trading coverage V for utility U starting from the maximum coverage, and (*bottom*) at the boundary of the $Q(n, l, \upsilon)$ solutions (see the Appendix) where the lifetime L is traded for coverage V. In [7], we show other examples where the dynamic programming solutions are compared with efficient solution algorithms based on continuous relaxations. Moreover, conditions are given to reduce the feasibility set of the

sensors to improve the computational demand of the dynamic programming solution.

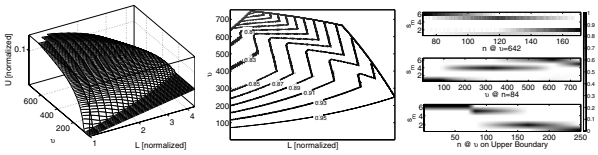

(a) (b) (c)

Figure 5. (a) Pareto efficient frontier (b) Constant reliability contours (c) Resource distribution for various paths on (a). Darker colors imply more resources.

Cost and Effects of Mobility To have a basic understanding of how mobility improves the Pareto frontier of a sensor network, let us consider a three sensor type pool with the GNS strategy with $q = 4$ where the sensors characteristics lead to $f_t = m^2$. Furthermore, $\boldsymbol{c} = [\ 3, \quad 4, \quad 7\ ]$, $N_o = 2$, $\delta = 1.2$, and $a = 0$. Let us assume that we can buy a platform that can mobilize the sensors at a fixed cost of c_{mobility}. For the sake of simplicity, we assume that the lifetime of the mobile sensors is also communication limited.

For this simulation, the relevant typical numbers in (36) are $\varepsilon_{\text{g},4}^{\text{median}}$ and $\varepsilon_{\text{g},8}^{\text{median}}$, which have an approximate ratio of 1.5. Hence, we can extend the sensor network to $T = 6$ types with $f_{4,5,6} = q \times N_o \times f_{1,2,3} = 3 \times f_{1,2,3}$ with the respective costs of $c_{4,5,6} = c_{\text{mobility}} + c_{1,2,3}$. Figure 6 shows the Pareto frontier of U and L for stationary sensors alone (dotted line), mobile sensors alone (dashed line), and their combination when $c_{\text{mobility}} = 10$. As seen in the figure, by spending money on mobility, it is possible to simultaneously improve both U and L. In this case, it can be shown that the mobile sensors become infeasible when $c_{\text{mobility}} > 20$ using the dominating sensor pairs concept introduced in [7].

7 Conclusions

This paper develops a theory to predict the localization performance of a heterogeneous sensor network where the operation of the network exploits sensor management to conserve energy. The theory also accommodates mobile nodes operating in a search mode and leads to a maximization of a localization utility that is equivalent to the maximization of a weighted sum of the number of nodes of each sensor type in the network. This utility fits nicely into our previous work to determine the Pareto frontier of the sensor choices when determining the number of different types of sensors to deploy. It is demonstrated that the network design for stationary nodes need not have advanced knowledge of the class of sensor management techniques that provide optimal choices of a constant number of active nodes per snapshot. Furthermore, the sensor network design need not worry whether the sensor provides a range or bearing.

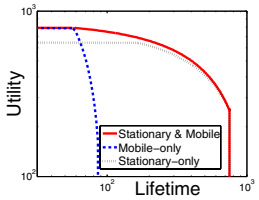

Figure 6. Pareto efficient frontier of U and L.

This paper lays down a theoretical justification of the localization utility under a number of assumptions. Future work will investigate whether many of these assumptions can be relaxed. For instance, is the sensor network design agnostic of any sensor management strategy that may select a variable number of active nodes per snapshot? Furthermore, many of the objectives are tightly coupled than modeled in this paper. For instance, the operation of the mobile node changes actually changes the lifetime objective because it needs to account for the energy to be mobile and the fact that mobile nodes could replenish their energy reserves easier than stationary nodes.

8 Acknowledgements

The authors would like to acknowledge Prof. Arkadi Nemirovsky, Prof. I. Volkan Isler, and Prof. Rama Chellappa for their insight and useful discussions.

References

[1] E. Altman and D. Miorandi. Coverage and connectivity of ad–hoc networks in presence of channel randomness. In *INFOCOM*, 2005.

[2] K. L. Bell, Y. Ephraim, and H. L. Van Trees. Explicit Ziv-Zakai lower bound for bearing estimation. *IEEE Transactions on Signal Processing*, 44(11):2810–2824, 1996.

[3] C. Bettstetter. On the minimum node degree and connectivity of a wireless multihop network. In *MOBIHOC 2002*, pages 80–91, EPF Lausanne, Switzerland, June 9-11, 2002.

[4] M. Bhardwaj and A. P. Chandrakasan. Bounding the lifetime of sensor networks via optimal role assignments. In *INFOCOM 2002*, volume 3, 2002.

[5] B. Bollobás. *Modern Graph Theory*. Springer Verlag, 1998.

[6] S. P. Boyd and L. Vandenberghe. *Convex Optimization*. Cambridge University Press, 2004.

[7] V. Cevher, L. Kaplan, and R. Chellappa. Acoustic sensor network design for position estimation. submitted to *ACM Trans. on Sensor Networks*, July 2007.

[8] L. Feeney and M. Nilsson. Investigating the energy consumption of a wireless network interface in an ad hoc networking environment. In *INFOCOM 2001*, volume 3, 2001.

[9] W. B. Heinzelman, A. P. Chandrakasan, and H. Balakrishnan. An application-specific protocol architecture for wireless microsensor networks. *IEEE Transactions on Wireless Communications*, 1(4):660–670, 2002.

[10] A. Howard, M. J. Mataric, and G. S. Sukhatme. Mobile sensor network deployment using potential fields: A distributed, scalable solution to the area coverage problem. *Distributed Autonomous Robotic Systems*, 5:299–308, 2002.

[11] C. Intanagonwiwat, R. Govindan, and D. Estrin. Directed diffusion: A scalable and robust communication paradigm for sensor networks. In *MOBICOM*, pages 56–67, 2000.
[12] L. M. Kaplan. Local node selection for localization in a distributed sensor network. *IEEE Trans. on Aerospace and Electronic Systems*, 1:136–146, Jan. 2006.
[13] L. M. Kaplan and V. Cevher. Design considerations for a heterogeneous network of bearings-only sensors using sensor management. In *Proc. of the IEEE/AIAA Aerospace Conference*, Big Sky, MT, Mar. 2007.
[14] L. M. Kaplan and Q. Le. On exploiting propagation delays for passive target localization using bearings-only measurements. *Journal of Franklin Institute*, pages 193–211, 2005.
[15] L. Lazos and R. Poovendran. Stochastic coverage in heterogeneous sensor networks. *ACM Trans. Sen. Netw.*, 2(3):325–358, 2006.
[16] E. L. Lehmann and G. Casella. *Theory of Point Estimation*. Springer, 1998.
[17] J. Liu, J. Reich, and F. Zhao. Collaborative in-network processing for target tracking. *EURASIP Journal on Applied Signal Processing*, 2003(4):378–391, Mar. 2003.
[18] S. Madden, M. Franklin, J. Hellerstein, and W. Hong. TAG: a Tiny AGgregation Service for Ad-Hoc Sensor Networks. In *Proceedings of the ACM Symposium on Operating System Design and Implementation*, 2002.
[19] R. Mathar and J. Mattfeldt. On the distribution of cumulated interference power in Rayleigh fading channels. *Wireless Networks*, 1:31–36, Feb. 1995.
[20] M. D. Penrose. On k-connectivity for a geometric random graph. *Random Structures and Algorithms*, 15(2), 1999.
[21] S. M. Ross. *Introduction to Probability Models*. Academic Press, San Diego, CA, eighth edition, 2003.
[22] D. K. Wilson. Atmospheric effects on acoustic arrays: A broad perspective from models. In *Proc.of the Meeting of the IRIA Specialty Group on Battlefield Acoustics and Seismics*, pages 39–51, Laurel, MD, Sept. 1999.
[23] D. K. Wilson, B. M. Sandler, and T. Pham. Simulation of detection and beamforming with acousitcal ground sensors. In *Proc. of SPIE*, volume 4743, pages 50–61, 2002.
[24] H. Zhang and J. Hou. On deriving the upper bound of α-lifetime for large sensor networks. In *Proceedings of the 5th ACM International Symposium on Mobile Ad Hoc Networking and Computing*, pages 121–132, 2004.

A Dynamic Programming Solution

Table 1 summarizes our dynamic programming algorithm that can solve the **Design Problem**. This solution provides a framework for decomposing the problem into a nested family of subproblems, denoted as $Q(n, l, \upsilon)$, where n allows us to enumerate the feasible total number of design vectors whereby determining the lifetime L, l explores their corresponding utility space whereby establishing U, and υ calculates the corresponding coverage space. The nested structure Q is implemented using a recursive approach for solving the original problem from the solutions of the subproblems. Hence, in Table 1, we determine a sequential decision process that provides necessary conditions for optimality that the remaining decisions in the recursion must satisfy. As a result, the running time of the algorithm is pseudo-polynomial.

Table 1. Dynamic Programming Solution

Assume that f_m's and r_m's are integers in appropriately chosen scale, and let f^* and r^* be the largest of these integers, respectively. Also, let N^* be the largest $\sum_m n_m$ allowed by the cost constraint $\boldsymbol{c}'\boldsymbol{n} \leq \$$. Given integers n, $1 \leq n \leq N^*$, l, $1 \leq l \leq L = f^*N^*$, and υ, $1 \leq \upsilon \leq \Upsilon = r^*N^*$ consider the problem

$$Q(n, l, \upsilon) = \min_{\boldsymbol{n}} \left\{ \sum_m c_m n_m : \sum_m n_m = n, \sum_m f_m n_m = l, \sum_m r_m n_m = \upsilon \right\}. \tag{37}$$

We build optimal solutions to all feasible problems $Q(n, l, \upsilon)$ with $1 \leq n \leq N^*$, $1 \leq l \leq L$, and $1 \leq \upsilon \leq \Upsilon$ as follows:

1. ***Initialization***: Start with solving problems $Q(1, l, \upsilon)$'s for $l = 1, \ldots, L$ and $\upsilon = 1, \ldots, \upsilon$. Each problem can be solved by inspecting all T candidate solutions of *one of n_i's is 1, remaining n_i's are zeros*. In fact, to solve all these problems, it suffices to look at M candidate solutions only once. Indeed, in the beginning, let us assign all problems $Q(1, l, \upsilon)$ with empty feasible solution and guess $+\infty$ for the optimal value. Now, when looking one by one at solutions $(n_1 = 1,\ n_2 = \ldots = n_T = 0)$, $(n_1 = 0, n_2 = 1,$ $n_3 = \ldots = n_T = 0)$, …, $(n_1 = \ldots = n_{T-1} = 0,\ n_T = 1)$, we determine the problems from the family $Q(1, l, \upsilon)$ for each l and υ, for which the current solution is feasible. If the value of the objective at this solution is better than the one that the problem was equipped with, we replace the previous feasible solution of the problem, if any, with the current one and update the guess for problem's optimal value accordingly. As a result, we solve problems $Q(1, l, \upsilon)$ with $\mathcal{O}(ML\Upsilon)$.
2. ***Recursion***: Assume that we already have solved all problems $Q(n, l, \upsilon)$ with $n \leq k$ at l and υ, and have assigned these problems with optimal values and optimal solutions. To solve problems $Q(k+1, l, \upsilon)$, we look at, one after another, T candidate correction directions: $(d_1 = 1,\ d_2 = \ldots = d_T = 0)$, $(d_1 = 0,\ d_2 = 1, d_3 = \ldots = d_T = 0)$, …, $(d_1 = \ldots = d_{T-1} = 0, d_T = 1)$ and note the following: a feasible solution $\bar{\boldsymbol{n}} = [\ n_1 \quad n_2 \quad \ldots \quad n_T\ ]$ to $Q(k+1, l, \upsilon)$ is obtained by the correction in question. Order the correction's number in m so that the correction is increasing in n_m by 1 from a collection $\bar{\boldsymbol{n}}' =$ $[\ n_1 \quad n_2 \quad \ldots \quad n_{m-1} \quad n_m - 1 \quad n_{m+1} \quad \ldots \quad n_T\ ]$. In order for $\bar{\boldsymbol{n}}$ to be feasible for $Q(k+1, l, \upsilon)$, $\bar{\boldsymbol{n}}'$ should be feasible for $Q(k, l - f_m, \upsilon - r_m)$, and the cost of $\bar{\boldsymbol{n}}$ is the cost of $\bar{\boldsymbol{n}}'$ plus c_m. Then, we first assign all these problems with empty solutions and guesses $+\infty$ for the optimal value. We look at, one by one, the corrections d_m, and for every correction, look at the feasible problems $Q(k, l, \upsilon)$, $l = 1, \ldots, L$. When looking at d_m and $Q(k, l, \upsilon)$, we increase the mth component of the optimal solution of $Q(k, l, \upsilon)$ by 1, whereby getting a feasible solution to the problem $Q(k+1, l + f_m, \upsilon + r_m)$. If the cost of this solution $\bar{\boldsymbol{n}}$ is less than the current guess for the optimal value of the latter problem, we replace the current feasible solution assigned to $Q(k+1, l + f_m, \upsilon + r_m)$ with $\bar{\boldsymbol{n}}$ and update the guess for the optimal value accordingly. As a result, we obtain optimal solutions to all feasible problems $Q(k+1, l, \upsilon)$, $l = 1, \ldots, L$ and $\upsilon = 1, \ldots, \Upsilon$ with $\mathcal{O}(ML\Upsilon)$.
3. ***Wrap-up***: Repeating the above process, we solve all $Q(n, l, \upsilon)$ for $n \leq N^*$ with $\mathcal{O}(N^*ML\Upsilon) = \mathcal{O}(N^{*3}Mf^*r^*)$. The optimal solution to the NDS problem can be found by searching through the $Q(n, l, \upsilon)$-problems with the optimal value less than or equal to $\$$ and selecting among their optimal solutions the one with the largest objective value satisfying the coverage constraint.